Wideband Antenna Arraying Over Long Distances

Alberto Torre Fernández*

ABSTRACT. — Antennas separated by long distances have large delays and delay rates among them. If wide-bandwidth signals are received, frequency domain beamformers based on filter banks can be used to carry out signal combination. A new scheme based on subband delay compensation is proposed in this article. The main advantages of this scheme are the wider field of view of the array, the reduction of distortion in the transfer function, and the simplification of communications among sites. In order to perform coherent combination, the delay and delay rates need to be estimated. In order to do so, an algorithm is devised to estimate the differential phase, delay, and delay rate between two antennas based on the subband signals. This algorithm is first developed for a stationary case, in which the delay rate is zero. The product of subband signals is averaged and an inverse discrete Fourier transform (IDFT) is carried out to yield an estimate of the cross-correlation. For the nonstationary case, first the delay rate is calculated by means of a two-dimensional IDFT, and from that point a function similar to the one in the stationary case is obtained so as to compute the delay and phase offset.

I. Introduction

Satellite communication ground segments made up of arrays of parabolic antennas are characterized by having a large delay among antenna elements as compared to other types of phased arrays. Because of this, it is necessary to adjust the delay before phase compensation even though the signal has a moderate bandwidth. Additionally, if the antennas to be combined are not in the same location, the delay rate can also be very large and will have to be compensated as well. The maximum delay between two antennas on Earth pointing towards a deep-space probe occurs when both antennas are separated by a spherical angle equal to 90 deg; one of them is pointing at the horizon and the other at zenith. The geometric delay can be calculated as $\tau_g = \mathbf{B} \cdot \mathbf{u}/c$, where $\mathbf{B}$ is the baseline vector and $\mathbf{u}$ is the direction to the signal source. Under these circumstances, the maximum delay is $\tau_{\max} = R_{Earth}/c = 21$ milliseconds (ms). The delay rate can be calculated as $\tau'_g = \mathbf{B}' \cdot \mathbf{u}/c$, which, for a deep-space probe, is $\tau'_g = (\boldsymbol{\omega} \times \mathbf{B}) \cdot \mathbf{u}/c$, where $\boldsymbol{\omega}$ is the angular velocity vector

* Development Engineer, Madrid Deep Space Communications Complex, Spain; Ph.D. candidate, Department of Signals, Systéms and Radiocommunications, Polytechnical University of Madrid.

The research described in this publication was carried out under a contract with the National Aeronautics and Space Administration.

of the rotation of Earth, $|\boldsymbol{\omega}| \simeq 7.3 \times 10^{-5}$ rad/s. When two antennas are at diametrically opposed points, the delay rate between them is maximum and equal to $\tau'_{\max} = 2\omega R_{Earth}/c = 3.1$ μs/s.

If the received signal is narrowband, the effect of the delay rate can be approximated by a differential Doppler shift among antennas in the array [1]:

$$\Delta f_{Doppler} = \tau' \Omega_{RF}. \tag{1}$$

Equation (1) indicates that the Doppler frequency shift equals the product of the delay rate and the received frequency. The cross-ambiguity function (CAF) equation can be used to calculate both the delay and the delay rate:

$$CAF(\tau, \tau') = \int_0^\infty \tilde{x}_p(t)\tilde{y}_p^*(t-\tau)\exp(-j2\pi\tau'\Omega_{RF}t)dt. \tag{2}$$

Through calculation of the CAF of two antennas' received signals, and according to the peak position of the CAF, the delay and delay rate are achieved. As noted previously, the model in Equation (1) is an approximation only valid for narrowband signals or very low delay rates. In the more general case, the effect of the delay rate in the signal is the multiplication of the transform by the term $e^{-j\omega\tau' t}$. According to this term, each frequency will have a different equivalent Doppler frequency; the difference in Doppler frequency across band is equal to $BW \cdot \tau'$. For instance, for a delay rate equal to 10^{-9} and a bandwidth of 100 MHz, only 0.1 Hz of difference across band will exist. If the delay rate is increased to 10^{-6}, that difference will amount to 100 Hz. Another way of looking at the problems that arise when high delay rates are involved is by taking a look at the delay. With the same delay rate of 10^{-6} and $BW = 100$ MHz , it is necessary to use a temporal window of at least 0.01 s in order to have a frequency resolution of 100 Hz. During these 0.01 s, at least $2 \cdot 10^6$ samples will have been taken, which means that from the beginning of the window until the end, a slip of two samples will have occurred. Therefore, the delay estimated by Equation (2) will be not be accurate.

Nowadays, subband beamformers are being proposed to combine signals in arrays of parabolic dishes [2]. When working with subband beamformers, the CAF can be applied at the signals prior to subband decomposition or to the subband signals after the analysis filters. The former case is difficult to implement in hardware due to the high sampling rate of the fullband signal. Additionally, when high delay rates are involved, the frequency resolution is limited to the maximum delay shift in the analysis window. The latter case has an easier hardware implementation, but it can only be applied to the signals inside each subband without taking advantage of the information in the rest of the subbands; hence, it will be less accurate.

In order to circumvent these problems, the aim of this article is to find an algorithm that can estimate the phase, delay, and delay rate between two antennas from the joint subband signals under scenarios of high delay rates. In addition, an arraying scheme is proposed that compensates for the differential delay, delay rate, and phase among faraway ground stations.

II. Signal Model

Consider the following model [3] for a waveform incident on a reference point $\mathbf{r}_p$:

$$S_p(\Omega) = \int_{-\infty}^{\infty} S(\Omega')e^{-j\Omega\tau_p(t)}\delta(\Omega - \Omega_c - \Omega')d\Omega' = S(\Omega - \Omega_c)e^{-j\Omega\tau_p(t)}, \tag{3}$$

where $S(\Omega)$ is the Fourier transform of $s(t)$, the complex baseband representation of $s^{(RF)}(t)$, and $\tau_p(t)$ is given by

$$\tau_p(t) = \frac{\hat{\mathbf{u}}(t) \bullet \mathbf{r}_p}{c}, \tag{4}$$

where $\hat{\mathbf{u}}(t)$ is the unit magnitude vector that points from $\mathbf{r}_p$ towards the source, and c is the speed of light. As $\tau_p(t)$ varies with time, a Doppler shift appears that is due to the motion of the p^{th} element of the array with respect to a frame of reference that is fixed to the source in the far field ($zero^{th}$ element). In the case of deep-space probes, the main component of this motion is due to the rotation of Earth.

The output of the p^{th} array element is modeled as $G_p(\Omega;\hat{\mathbf{u}}(t))S_p(\Omega)$, where $G_p(\Omega;\hat{\mathbf{u}}(t))$ is the frequency response of the antenna in the direction of $\mathbf{u}(t)$. Next, the receiver shifts the source spectrum to baseband by mixing the incoming signal with a local oscillator (LO) frequency Ω_{LO}. The effects in the transfer function due to cables, amplifiers, and downconverters can be modeled as a single receiver-dependent baseband frequency response $C_p(\Omega)$. In summary, the measurement by the p^{th} receiver can be modeled as

$$V_p(\Omega) = C_p(\Omega - \Omega_c)G_p(\mathbf{u}(t),\Omega)S_p(\Omega) = C_p(\Omega - \Omega_c)G_p(\mathbf{u}(t),\Omega)e^{-j\Omega\tau_p(t)}S(\Omega - \Omega_c), \tag{5}$$

where $\tau_p(t) = \tau_p^c + \tau_p' t$, i.e., a constant term τ_p^c plus a linear time variation $\tau_p' t$. After mixing the RF signal with an LO with frequency Ω_{LO}, the signal at IF is

$$V_p^{IF}(\Omega) = C_p(\Omega - \Omega_{IF})G_p(\Omega + \Omega_{LO};\hat{\mathbf{u}}(t))S(\Omega - \Omega_{IF})e^{-j(\Omega+\Omega_{LO})\tau_p(t)}. \tag{6}$$

If the signal is now digitized and assuming equal antenna responses, the spectrum of the digital signal at IF can be shown to be

$$V_p^{IF}(\omega) = X(\omega - \omega_{IF})e^{-j\Omega_{LO}\tau_p^c}e^{-j\omega\Delta_p^c}e^{-jd_p^{IF}n}e^{-j\omega\tau_p' n}, \tag{7}$$

where $X(\omega - \omega_{IF})$ is the discrete time Fourier transform equivalent of the analog baseband transfer function $C(\Omega - \Omega_{IF})G(\Omega + \Omega_{LO};\hat{\mathbf{u}}(t))S(\Omega - \Omega_{IF})$, $d_p^{IF} = \Omega_{LO}\tau_p' / f_s$ is the Doppler frequency due to the delay rate, and $\Delta_p^c = \tau_p^c / T_s$. By carrying out a digital second downconversion to baseband, the resulting signal is

$$X_p(\omega) = X(\omega)e^{-j\Omega_c\tau_p^c}e^{-j\omega\Delta_p^c}e^{-jd_p n}e^{-j\omega\tau_p' n}, \tag{8}$$

where $d_p = \frac{\omega_c\tau_p'}{f_s}$ is the differential Doppler frequency with the signal at baseband. If the signal $X_p[n] \xleftrightarrow{\mathcal{F}} X_p(\omega)$ goes through a uniform modulated filter bank with prototype filter $h[n]$, K bands, and M decimation ratio, the signal at band k can be represented as [4]

$$X_{p,k}[m] = W_K^{-kmM} \underline{X}_{p,k}[m] \tag{9}$$

where $\underline{X}_{p,k}$ is the short-time Fourier transform of $x_p[n]$:

$$\underline{X}_{p,k}[m] = \sum_{n=-\infty}^{\infty} h[mM-n] W_K^{k(mM-n)} x_p[n]. \tag{10}$$

This short-time Fourier transform can be interpreted as the result of passing the signal through a filter $H_k(\omega) = H\left(\omega - \frac{2\pi}{K}k\right)$ and decimating by a factor M the output of the signal. If the prototype filter $h[n]$ is selective enough, and in addition oversampling is used, the alias components can be discarded, i.e.,

$$\mathcal{F}\left\{\underline{X}_{p,k}[m]\right\} \simeq H_k\left(\frac{\omega}{M}\right) X_p\left(\frac{\omega}{M}\right). \tag{11}$$

After modulating $\underline{X}_{p,k}[m]$ by W_K^{-kmM}, the result is

$$\begin{aligned} X_{p,k}^{SB}(\omega) &\simeq H\left(\frac{\omega}{M}\right) X_p\left(\frac{1}{M}\left(\omega + \frac{2\pi k}{K}M\right)\right) \\ &= H\left(\frac{\omega}{M}\right) X\left(\frac{\omega}{M} + \frac{2\pi k}{K}\right) e^{-j(\Omega_c \tau_p^c + \frac{2\pi k}{K}\Delta_p^c)} e^{-j\omega\frac{\Delta_p^c}{M}} e^{-j\left(d_p + \frac{2\pi k}{K}\tau_p'\right)n} e^{-j\omega\frac{\tau_p'}{M}n} \end{aligned} \tag{12}$$

The different terms in Equation (12) are:

- $e^{-j\left(\Omega_c \tau_p^c + \frac{2\pi k}{K}\Delta_p^c\right)}$. There is a phase ramp across the whole band equal to $\angle T(k) = \frac{2\pi k}{K}\Delta_p^c$; observe that the IDFT of $T(k)$ is the $\delta[m - \Delta_p^c]$.
- $e^{-j\omega\frac{\Delta_p^c}{M}}$. This is the Fourier transform of $\delta\left[m - \frac{\Delta_p^c}{M}\right]$, and it is obviously due to the delay of $\frac{\Delta_p^c}{M}$ samples at each subband.
- $e^{-j\left(d_p + \frac{2\pi k}{K}\tau_p'\right)n}$. The phase rotation is also dependent on the subband number. This is because the filterbank effects a third downconversion on those bands with $k > 0$. It must be taken into account that n is the full band sample number prior to decimation, and $m = \frac{n}{M}$ is the subband sample number. If we use the decimated sample number m instead of n, the result is that of increasing the frequencies by a factor of M, i.e., $e^{-j\left(d_p M + \frac{2\pi k}{K}(\tau_p' M)\right)}$.
- $e^{-j\omega\frac{\tau_p'}{M}n}$. This term reflects the effect of the delay rate on the subband. Observe that this can also be expressed as $e^{-j\omega\tau_p' m}$, i.e., the delay rate is also τ_p' at the subband level.

III. Arraying Scheme

All the exponential terms in Equation (12) can be compensated by multiplying the signal by their corresponding complex conjugate or delaying it by the appropriate amount. If the antennas are in different locations, sending the phase and delay values to each of the antennas can be very difficult due to synchronization issues. It is better to send all the digitized data to a central site, where correlation and coherent combining is done jointly for all of the antennas. The transmission of the data can be done more effectively once each of the signals has been decomposed into subbands (Figure 1). In this way, the synchronization accuracy among the different streams of data can be reduced by a factor equal to the deci-

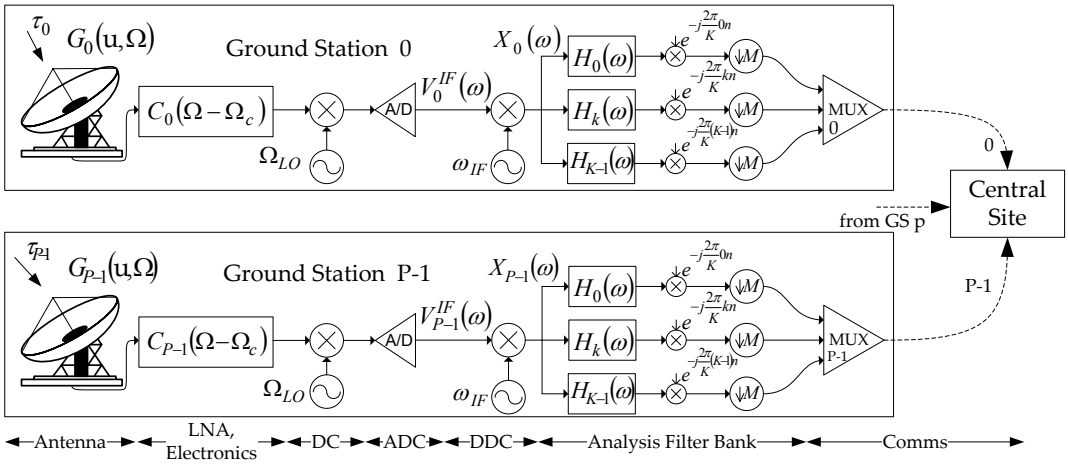

Figure 1. Remote site subband decomposition.

mation ratio, as the data that need to be aligned are the subband samples. If the samples coming out of the analog-to-digital converters were sent directly, the jitter in the clocks and communication lines would cause the samples to jump from one time slot to another. This would be equivalent to a time-varying delay that should be compensated by subsequent stages. For instance, if the sampling period is equal to 1 nanosecond (ns), and the clocks and communication lines are synchronized by GPS, jitters on the order of several tens of nanoseconds can be expected. With a decimation ratio equal to 100, the required synchronization accuracy is on the order of 0.1 ms, so it is very unlikely that a subband sample will fall in an erroneous time slot. Another advantage of this scheme is that in the case of working with narrowband signals, only those subbands with signals inside should be sent, with the consequent reduction in costs.

Once in the central site, all links coming from the remote ground stations are first demultiplexed. Then, one of the ground stations is chosen as reference one (ground station zero in Figure 2), and the rest of the antennas are correlated with regard to this one in order to find the values of τ_p' (delay rate), Δ_p initial delay in samples, and ϕ_p (phase offset). In total, *P*–1 correlator units are required. Once this triplet of values is estimated for each of the ground stations, the subbands have to be equalized by compensating them in frequency $\omega_{p,k}^{SB} = d_p + \frac{2\pi k}{K}\tau_p'$, delay $\Delta_{p,k}^{SB} = \frac{\Delta_p^c}{M} + \tau_p'\ m$, and phase $\phi_{p,k}^{SB} = \Omega_c \tau_p^c + \frac{2\pi k}{K}\Delta_p^c$. This is done by means of *P*–1 equalizer units; as ground station zero is reference one, no equalization is required for this ground station. Frequency compensation is done by a numeric control oscillator, and phase compensation by a complex multiplier. Delay compensation can be performed by the series of a coarse delay buffer and a fractional delay filter. The coarse delay buffer will implement the integer part of the delay $\left\lfloor \Delta_{p,k}^{SB} \right\rfloor$ and the fractional delay filter [5] the remainder $\Delta_{p,k}^{SB} - \left\lfloor \Delta_{p,k}^{SB} \right\rfloor$. For example, if the delay goes from 1.98 to 2.02 samples in 0.01 steps, the coarse delay buffer will be set at [1 1 2 2 2] samples and the fractional delay filter at [0.98 0.99 0 0.01 0.02] samples.

Once equalization is made and if no other distortions are present, the signals at each of the subbands can be added. However, the group delay at each ground station will be different, due mainly to electronics and cables. Therefore, a second stage is required to account for

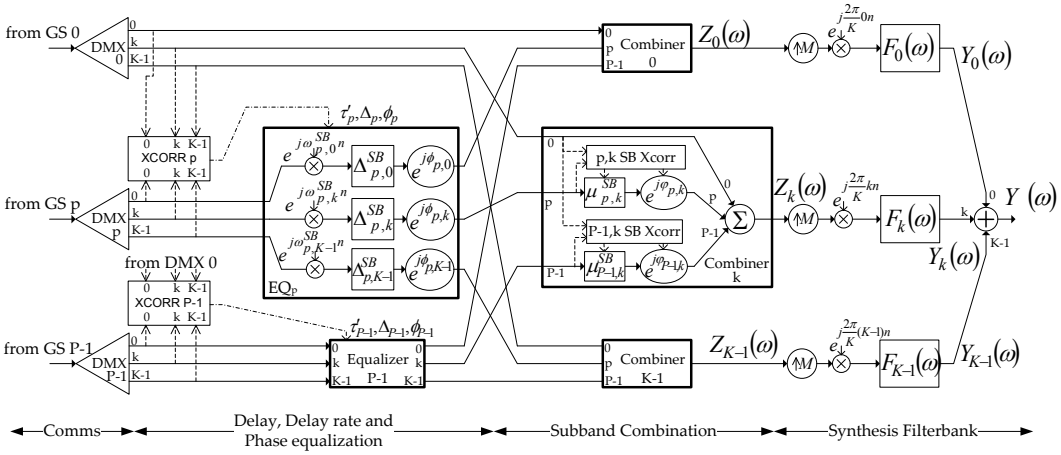

Figure 2. Central site equalization and combination.

these imbalances. In this second stage, only phase $\varphi_{p,k}^{SB}$ and delay $\mu_{p,k}^{SB}$ need to be adjusted. The frequency and delay rates have already been compensated in the equalization stage. The residual estimation errors in frequency and delay rate will be accounted for by the successive phase and delay estimations in the second stage. For this purpose, a correlator that deals with the complex signal can be used to estimate the residual phase and delay offsets due to group delay imbalances [6]. As it is not expected to have delay offsets larger than one sample, a fractional delay filter is enough to carry out the compensation. Successive delay and relay rate estimations will make it possible to compensate the second derivative of the delay.

The correlation that takes place in the first stage (XCORR p units) can take some milliseconds, as shown in Section V. During this time, no combination will be possible in the second stage, as the high differential Doppler among ground stations will render subband correlation very difficult. For instance, if $\tau_p' = 10^{-6}$ and $f_c = 8$ GHz, then $d_p = 2\pi \times 8 \times 10^3$ rads/s. If the subband sampling frequency is 10^6 samples/s, the phase drift will be equal to 2.88 deg/sample.

A. Beam Squint

Other arraying schemes only deal with frequency and phase compensation inside the subbands. The delay compensation is carried out by means of a coarse delay buffer before subband decomposition. The first limitation of a scheme such as that appears when there are group delay ripples higher than one sample; only phase compensation inside the subbands will not be enough to equalize these ripples. Additionally, in such schemes beam squint is unavoidable. In order to quantify it, let us take a stationary ($\tau_p' = 0$) uniform linear array model with $\tau_p = (P-p)\frac{d}{c}\sin\theta$, where d is the interelement distance and θ is the angle of arrival. Suppose that at some angle θ_0, the coarse delay buffers are set at Δ_p. At the same time, assume that at some desired angle θ_r, the phase offsets among antennas are compensated with $\phi_{p,k} = \Omega_c((P-p)\frac{d}{c}\sin\theta_r) + \frac{2\pi k}{K}(\frac{1}{T_s}(P-p)\frac{d}{c}\sin\theta_r + \Delta_p)$. After adding all signals at each subband, the result is

$$Z_k^{CD}(\omega) = H\left(\frac{\omega}{M}\right)e^{-j\pi k(L-1)/K}X\left(\frac{1}{M}\left(\omega+\frac{2\pi k}{K}M\right)\right)e^{-j\left(\Omega_c+\frac{1}{T_s}\frac{2\pi k}{K}+\frac{1}{T_s}\frac{\omega}{M}\right)P\frac{d}{c}(u-u_r)}$$

$$\frac{1}{P}\frac{\sin\left(P\frac{d}{2c}\left(\left(\Omega_c+\frac{2\pi k}{K}\frac{1}{T_s}\right)(u-u_r)+\frac{\omega}{MT_s}(u-u_0)\right)\right)}{\sin\left(\frac{d}{2c}\left(\left(\Omega_c+\frac{2\pi k}{K}\frac{1}{T_s}\right)(u-u_r)+\frac{\omega}{MT_s}(u-u_0)\right)\right)}, \tag{13}$$

where $u_x = \sin\theta_x$. According to Equation (13), the beam pattern will depend on the subband number and the baseband frequency in that subband. To calculate the new pointing angle for the signal at subband k, the denominator is set equal to zero, yielding

$$\theta_k = \arcsin\left(\frac{\Omega_{ck}}{\Omega_{ck}-\Delta\Omega}u_r - \frac{\Delta\Omega}{\Omega_{ck}-\Delta\Omega}u_0\right), \tag{14}$$

where $\Omega_{ck} = \Omega_c + \frac{2\pi k}{K}\frac{1}{T_s}$ and $\Delta\Omega = \frac{\omega}{MT_s}$. The array pattern will be free of beam squint only if $k = 0$ and $\omega = 0$. Should the delay have been totally compensated as in Figure 2, the result would be

$$Z_k(\omega) = H\left(\frac{\omega}{M}\right)e^{-j\pi k(L-1)/K}X\left(\frac{1}{M}\left(\omega+\frac{2\pi k}{K}M\right)\right)e^{-j\left(\Omega_c+\frac{1}{T_s}\frac{2\pi k}{K}+\frac{1}{T_s}\frac{\omega}{M}\right)P\frac{d}{c}(u-u_r)}$$

$$\frac{1}{P}\frac{\sin\left(P\frac{d}{2c}\left(\left(\Omega_c+\frac{2\pi k}{K}\frac{1}{T_s}+\frac{\omega}{MT_s}\right)(u-u_r)\right)\right)}{\sin\left(\frac{d}{2c}\left(\left(\Omega_c+\frac{2\pi k}{K}\frac{1}{T_s}+\frac{\omega}{MT_s}\right)(u-u_r)\right)\right)}, \tag{15}$$

which is free of beam squint. Even though the scheme in Figure 2 is free of beam squint, the amount of beam squint in an array without subband delay compensation and with long distances among array elements is negligible. Only for short distances, as in Figure 3, is the beam squint significant.

B. Transfer Function

The impact of not compensating the term $e^{-j\omega\frac{\Delta_p}{M}}$ inside the subbands is more noticeable when observing the transfer function of the whole array. Under these circumstances, the input–output transfer function in the z-domain of a filter bank beamformer can be expressed as

$$Y(z) = \sum_{i=0}^{K-1} Y_i(z) = \sum_{i=0}^{K-1}\frac{1}{K}\left[\sum_{l=0}^{K-1} F_i(z)\sum_{p=0}^{P-1} H_\epsilon\left(\Phi, z^N, \epsilon_{p,l}\right)H_i\left(zW_K^l\right)X\left(zW_K^l\right)\right], \tag{16}$$

where $H_\epsilon\left(\Phi, z^N, \epsilon_{p,l}\right)$ is the z-transform of the delay not compensated at each subband. To model this uncompensated delay, and assuming it is lower than the subband sample time, a fractional delay filter can be used [7]. The transfer function of the fractional delay filter is

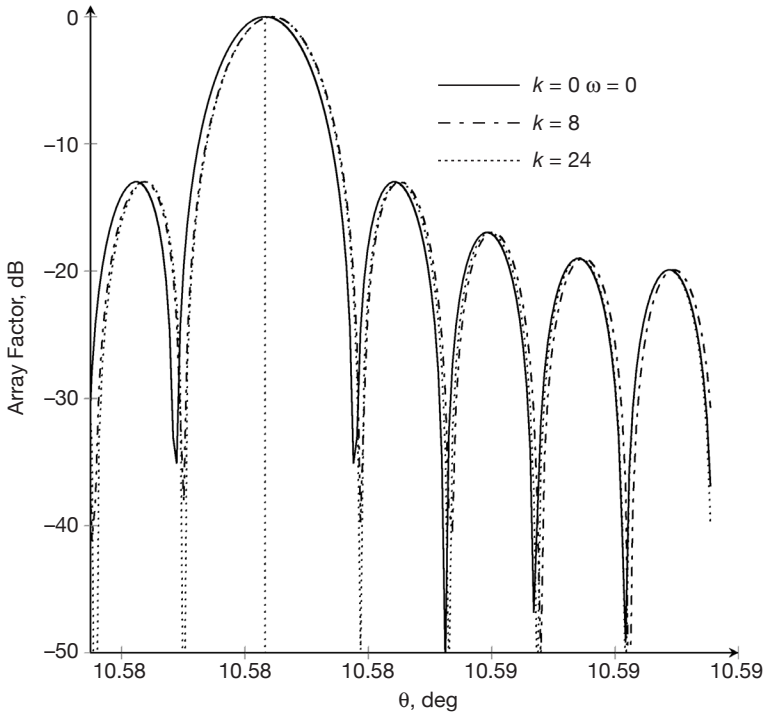

Figure 3. Beam squint for a 10-element antenna array, with θ_0 = 10 deg, θ_r = 10.582 deg, coarse delay buffer step = 10 samples, T_s = 5 ns, BW = 100 MHz, K = 32, and f_c = 8 GHz.

$$H_\epsilon(\Phi, z, \epsilon) = \sum_{n=0}^{2M-1} h_\epsilon(\Phi, n, \epsilon) z^{-n}, \tag{17}$$

where

$$h_\epsilon(\Phi, n, \epsilon) = g_0(n) + \sum_{l=1}^{L} g_l(n)(1-2\epsilon)^l \tag{18}$$

and Φ is the adjustable parameter vector given by

$$\Phi = \left[g_0(0)\ \ g_0(1)\ \ \ldots\ \ g_0(M-1)\ \ g_1(0)\ \ g_1(1)\ \ g_1(M-1)\ \ \ldots\ \ g_L(0)\ \ g_L(1)\ \ \ldots\ \ g_L(M-1)\right]. \tag{19}$$

The fractional delay $\epsilon_{p,l} = \epsilon\ \forall p > 0, \forall l$ is modeled as a Gaussian random variable with mean 0.5 (the input value to the fractional delay filter must be between 0 and 1) and variance σ_τ^2. Thus, the mean transfer function after adding up all antennas for each subband is

$$\overline{H}_\epsilon(\Phi, z, \epsilon) = \frac{1}{P}\sum_{n=0}^{2M-1} g_0(n) z^{-n} + \frac{P-1}{P}\sum_{n=0}^{2M-1}\left[g_0(n) + \sum_{l=1}^{L} g_l(n) E\left[(1-2\epsilon)^l\right]\right] z^{-n}. \tag{20}$$

The different moments for a fractional delay filter with $L = 4$ are $E[(1-2\epsilon)] = 0$, $E[(1-2\epsilon)^2] = 4\sigma_\tau^2$, $E[(1-2\epsilon)^3] = 0$, and $E[(1-2\epsilon)^4] = 48\sigma_\tau^4$. Therefore, the expected transfer function of the whole subband beamformer can be expressed as

$$\overline{H\epsilon}^{SB}(z) = E\left[\sum_{i=0}^{K-1} Y_i(z)\right]$$

$$= \sum_{i=0}^{K-1} \frac{1}{K} \sum_{i=0}^{K-1} F_i(z) H_i\left(zW_K^l\right)\left[\sum_{n=0}^{2M-1}\left[g_0(n) + \frac{P-1}{P}\left(4\sigma_\tau^2 g_2(n) + 48\sigma_\tau^4 g_4(n)\right)\right] z^{-nN}\right]. \tag{21}$$

If the coarse delay buffer step is set to one sample and the number of subbands is high, evaluation of Equation (21) does not show any important degradation. When working with antennas separated long distances apart, it is important to increase the coarse delay step so as to increase the field of view. Imagine two antennas separated by 30 km; changing the direction of arrival by 1 mdeg will change the coarse delay buffer by nearly 2 ns. Hence, if the coarse delay buffer is set at 2 ns, then it will be possible to acquire only those signals within ±1 mdeg. This is a very narrow field of view, taking into account that a 34-m antenna has a 3-dB beamwidth in X-band of approximately 70 mdeg. If the coarse delay step is increased to 10 ns (5 samples), the degradation caused by not compensating the subband delay can be seen in the dashed and dashed-dot lines of Figure 4. On the contrary, the continuous line, which corresponds to an array with subband delay compensation, shows very small ripple both in magnitude and phase. In both cases, a perfect reconstruction filter bank with linear phase analysis filters has been used [8].

With the scheme depicted in Figure 2, all differential delays are compensated within the subband. Therefore, the field of view can be as wide as the 3-dB beamwidth of each individual antenna. This can prove very useful when single aperture–multiple link schemes are used, as all of the spacecraft within the field of view of each individual antenna can be tracked.

IV. Delay Estimation in the Stationary Case

Take the signals at two antennas p and q, $x_p[n] = x[n - \Delta_p^c]$ and $x_q[n] = x[n - \Delta_q^c]$, that go through a filter bank with prototype filter $h[n]$. The subband decomposition of these signals ($i = p, q$) can be expressed as

$$X_{i,k}[n] = \sum_{r=-\infty}^{\infty} h[-r] x_i[r + nM] W_K^{-k(r+nM)}. \tag{22}$$

An analysis filter bank with K subbands can be interpreted as a K point spectrum estimator. The estimation of the cross-power spectral density can be obtained by averaging at each frequency point the product of the two signals' spectrum $\hat{\Gamma}_{x_p x_q}[k] = E\{X_p(k) X_q^*(k)\}$.[1] In the case of subband filters, the mean value of the output of each subband filter will be the spectrum of the input signal at that frequency. Hence, the expected value of the product of the subband signals will have a phase related to the phase difference between the spectrum of both antenna input signals:

[1] G. C. Carter, *Time Delay Estimation*, Ph.D. dissertation, University of Connecticut, 1976.

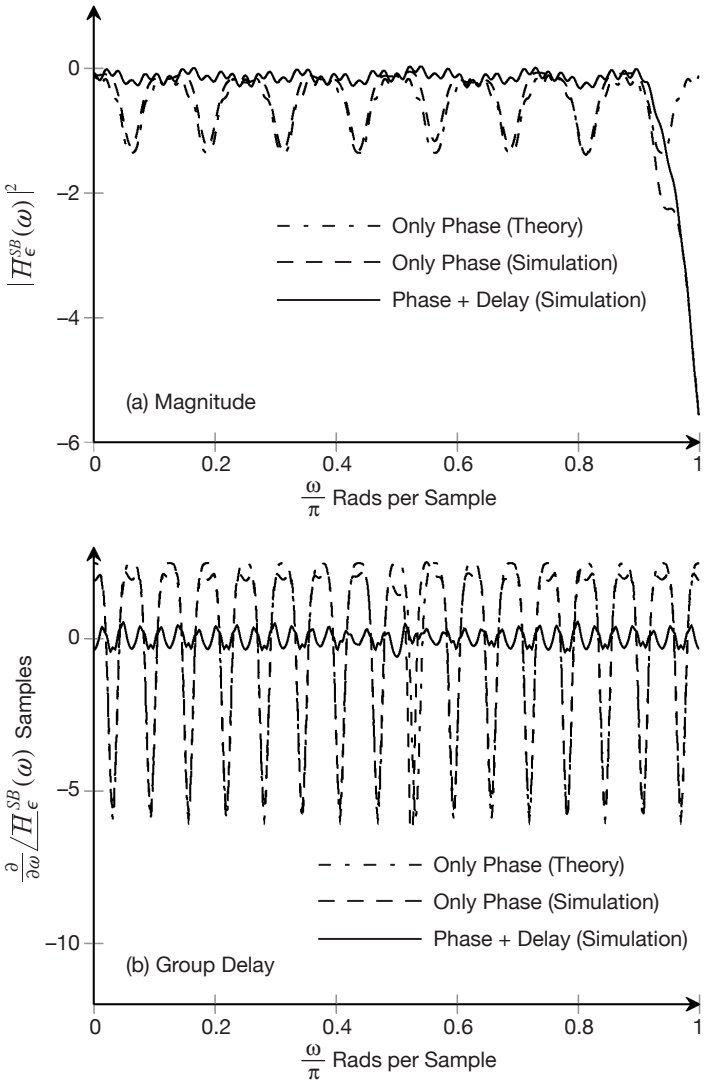

Figure 4. Transfer function comparison between beamformers with and without delay subband compensation for $P = 10$, $K = 16$, $N = K/2$, and $\sigma_\tau^2 = 1/N$ samples.

$$E\left\{X_{p,k}[n]X_{q,k}^*[n]\right\} = \sum_{r=-\infty}^{\infty}\sum_{l=-\infty}^{\infty} h[-r]h^*[-l]\gamma_{xx}[r-l]W_K^{-k(r-l)}W_K^{-k(\Delta_p-\Delta_q)}$$

$$= \left(\Gamma_{xx}[k]W_K^{-k(\Delta_p-\Delta_q)}\right) * \left|H[k]\right|^2. \tag{23}$$

Taking its inverse DFT yields

$$IDFT\left\{E\left\{X_{p,k}[n]X_{q,k}^*[n]\right\}\right\} = IDFT\left\{\left(\Gamma_{xx}[k]W_K^{-k(\Delta_p-\Delta_q)}\right) * \left|H[k]\right|^2\right\} = \gamma_{x_p x_q}[m]\gamma_{hh}[m]. \tag{24}$$

If the last expression is divided by $\gamma_{hh}[m]$, the cross-correlation among the two signals is obtained and any of the methods based on interpolation of the cross-correlation function can

be used to estimate the delay. The advantage of this method is that it can work with large delays and narrow bandwidths, and is relatively immune to spectral gaps, as opposed to the phase data method [9]. This advantage is due to the fact that this new method uses not only the phase information but also the magnitude information at all subbands. Another advantage is that it can work with a low number of subbands, unlike the phase method, whose accuracy is influenced greatly by the total number of subbands. Practical implementation of the method requires replacement of the $E\{\}$ operator by a temporal average

$$\hat{r}_{xy}[m] = \frac{IDFT\left\{\frac{1}{N}\sum_{n=0}^{N-1} X_k[n]Y_k^*[n]\right\}}{\gamma_{hh}[m]}. \tag{25}$$

In Figure 5, it can be seen how the cross-correlation obtained by this method is equal to the one obtained by the direct method, which works with the signals prior to subband decompositions.

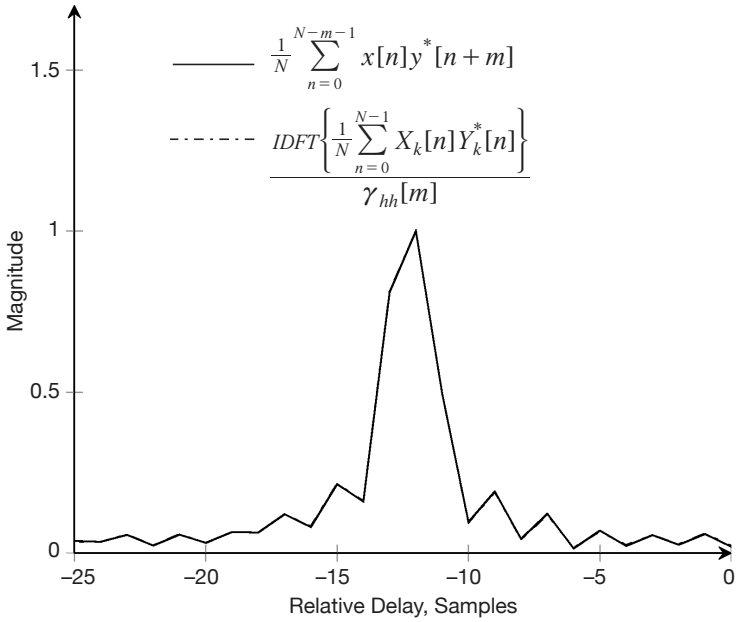

Figure 5. Cross-correlation from direct method and by cross-power spectral density inverse transform for a signal with B_n = 0.5, K = 64, and τ = 12.5.

In the case that the bandwidth of the signal is small, this method, unlike the phase data method, behaves properly, as seen in Figure 6.

Another important advantage when compared to the phase data method comes in terms of fastest convergence when working in low signal-to-noise (SNR) scenarios. To evaluate the accuracy of the method, the combining losses in arrays with different number of antennas are calculated. These combining losses arise due to inaccurate estimation of phase and

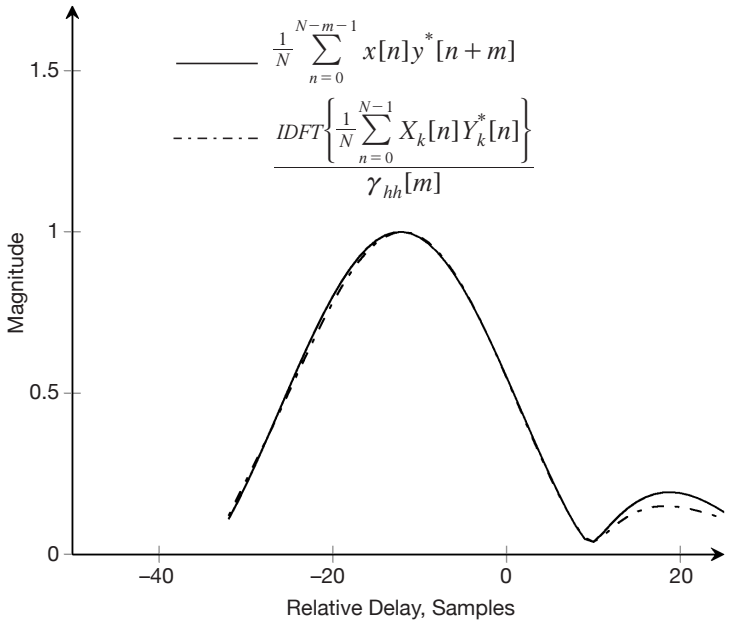

Figure 6. Cross-correlation from direct method and by cross-power spectral density inverse transform for a signal with B_n = 0.05, K = 64, and τ = –12.5.

delay. As seen in Figure 7, working at an SNR of –10 dB, convergence can be achieved with the subband cross-power spectral density inverse transform (SCPSDIT) method only with 256 samples per subband even for a large number of antennas.

V. Delay Estimation in the Nonstationary Case

Similar to the method developed in the previous section, an analysis of the cross-power spectral density of the subbands in a filter bank can be carried out so as to estimate the delay rate among two antennas. The parameters that need to be obtained are the delay and delay rate differences, i.e, $\Delta_{pq} = \Delta_p^c - \Delta_q^c$ and $\tau'_{pq} = \tau'_p - \tau'_q$. Using the time domain subband signals $x_{p,k}^{SB}[m]$ and $x_{q,k}^{SB}[m]$, and resorting to the development in Section II,

$$\Gamma_{p,q}^{SB}[k,m] = E\left[x_{p,k}^{SB}[m]\left(x_{q,k}^{SB}[m]\right)^*\right] = \left(\Gamma_{xx}[k]W_K^{k\left(\Delta_{pq}+\tau'_{pq}m\right)}\right) * |H[k]|^2. \tag{26}$$

The maximum likelihood estimate of the delay and delay rate can be calculated by maximizing the following function[2]:

$$\max_{\Delta,\tau'} \sum_m \sum_i X_p(\omega_i) X_q^*(\omega_i) e^{-j\omega_i(\Delta+\tau' m)}. \tag{27}$$

Replacing ω_i by the discrete subband frequency $2\pi k/K$, and taking expectation on the previous equation, the result is

[2] A. Whitney, *Precision Geodesy and Astrometry via Very-Long-Baseline Interferometry*, Ph.D. dissertation, Massachusetts Institute of Technology, 1974.

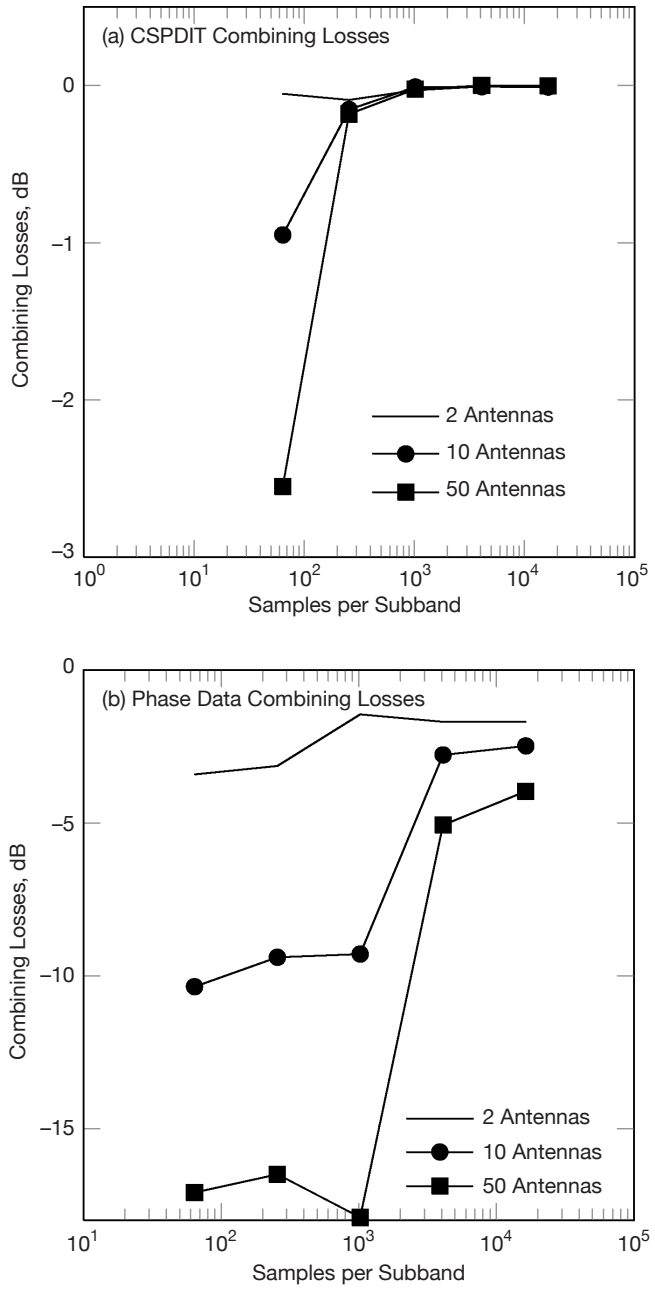

Figure 7. Comparison of convergence of SCPSDIT and phase data methods in a filterbank with $K = 64$, $M = 32$, $L = 256$, SNR = –10 dB, $B_n = 0.5$, and $\Delta_{max} = 1$ sample.

$$\left\langle \Delta_{pq}, \tau'_{pq} \right\rangle = \max_{\Delta,\tau'} \sum_{k} \sum_{m} \Gamma^{SB}_{p,q}[k,m] e^{-j\frac{2\pi k}{K}(\Delta+\tau' m)}. \tag{28}$$

Equation (28) is basically a two-dimensional DFT, so by rearranging the exponential terms, the search for the maximum can be efficiently done by the following 2D DFT:

$$\left\langle \Delta_{pq}, \tau'_{pq} \right\rangle = \max_{r,l} \sum_{k} \sum_{m} \Gamma^{SB}_{p,q}[k,m] e^{-j\frac{2\pi}{K}kr} e^{-j\frac{2\pi}{K}ml}$$

$$= \max_{r,l} \sum_{k} \left(\Gamma_{xx}[k] W_K^{k\Delta_{pq}} \delta\left[l - \tau'_{pq} M \frac{k}{K} \right] \right) * \left| H[k] \right|^2 e^{-j\frac{2\pi}{K}kr}. \quad (29)$$

Equation (29) is to be interpreted as follows: the 2D DFT over the temporal sequence $x^{SB}_{p,k}[m]\left(x^{SB}_{q,k}[m]\right)^*$ results in a two-variable function composed of the sum of K functions of the form $\Gamma_{xx}[k] W_K^{k\Delta_{pq}} * |H[k]|^2$ along the line defined in the plane l,k by $l = \tau'_{pq} M \frac{k}{K}$. Evaluation of Equation (29) along this line yields $\Gamma_{xx}[k] W_K^{k\Delta_{pq}} * |H[k]|^2$, which, after following the method developed in Section V, yields Δ_{pq}. The overall algorithm is described next.

Algorithm 1. Cross-power density 2-dimensional IDFT algorithm

Data: $x^{SB}_{p,k}[m]\, x^{SB}_{q,k}[m]$

Result: $\phi_{pq}, \Delta_{pq}, \Gamma'_{pq}$

begin

  for $k = 0$ **to** $K-1$ **do**

    $\upsilon^{SB}_{p,q}[k,m] = x^{SB}_{p,k}[m] \left(x^{SB}_{q,k}[m] \right)^*$

  end

  Compute 2-dimensional DFT

  $\Upsilon^{SB}_{p,q}[r,l] = \mathcal{F}\left[\upsilon^{SB}_{p,q}[k,m] \right] = \sum_k \sum_m \upsilon^{SB}_{p,q}[k,m] e^{-j\frac{2\pi}{K}kr} e^{-j\frac{2\pi}{L}ml}$

  for $r = 0$ **to** $K-1$ **do**

    $l_{\max}[r] = \max \Upsilon^{SB}_{p,q}[r,l]$

  end

  Perform regression analysis over the line $\mathbf{s}\ [r, l_{\max}]$

  $$\hat{\tau}'_{pq} = \frac{K}{M} \frac{\sum_{r=0}^{K-1} r \cdot l_{\max}[r]}{\sum_{r=0}^{K-1} r^2}$$

  Calculate cross-power density

  $\hat{\Gamma}_{p,q}[r] = \Upsilon^{SB}_{p,q}[r, l_{\max}(r)]$

  Calculate cross-correlation

  $\hat{\gamma}_{p,q}[m] = \mathcal{F}^{-1}\left[\hat{\Gamma}_{p,q}[r] \right]$

  Search for maximum of $\hat{\gamma}_{p,q}[m]$ and perform parabolic peak interpolation $\rightarrow \hat{\phi}_{pq}, \hat{\Delta}_{pq}$

end

The effect of the Doppler frequency d_{pq} is a shift in frequency, i.e., the new line is $l = \tau'_{pq} M\frac{k}{K} + d_{pq} M$. As in most cases, the delay rate is very small; the subband signals $x^{SB}_{p,k}[m]$ can be further decimated before carrying out the multiplication of subband signals. This is because the differential Doppler frequency $\Omega_c \tau'$ is very small in comparison with the sampling frequency f_s. In this way, the number of points to be stored can be reduced and the time to compute the 2D DFT reduced as well.

The overall procedure is illustrated in the following figures, which are the result of delaying a broadband signal modeled as Gaussian noise filtered at $\omega_n = 0.9\pi$. Figure 8 shows the contour plot of the 2D DFT in Equation (29). The line corresponding to variation of the differential Doppler across the subbands can be seen clearly.

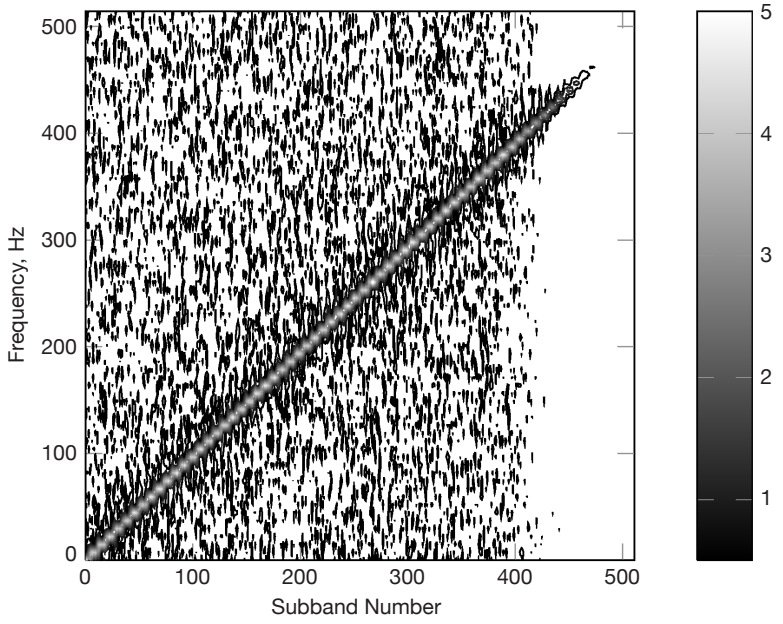

Figure 8. Contour plot of $\left|\sum_k \sum_m \Gamma^{SB}_{p,q}[k,m] e^{-j\frac{2\pi}{K}kr} e^{-j\frac{2\pi}{K}ml}\right|$. Initial delay Δ = 400 samples, τ' = 10^{-6}, f_s = 1 GHz, SNR = –10 dB, L = 2^{27} samples (0.125 s), K = 1024 subbands, and M = K/2.

Once the cross-power spectral density is evaluated along the line defined by the maximum values, the cross-correlation can be obtained by computing the inverse DFT. The result is shown in Figure 9, and as in Section IV, the cross-correlation has a clear peak at the value corresponding to the delay at the beginning of the data. Finally, the value of the phase is evaluated by carrying out a parabolic interpolation of the peak value.

The bias and standard deviation of the estimates of ϕ, τ, τ' have been computed by simulation for several values of SNR (Figure 10). In all cases, every point is the result of 50 executions. From the results, it can be gathered that phase and delay rates estimates are unbiased; the bias in delay estimation is due to the parabolic peak interpolation. It is worth pointing out the high accuracy of all estimates for low SNR, due mainly to the high number of samples involved.

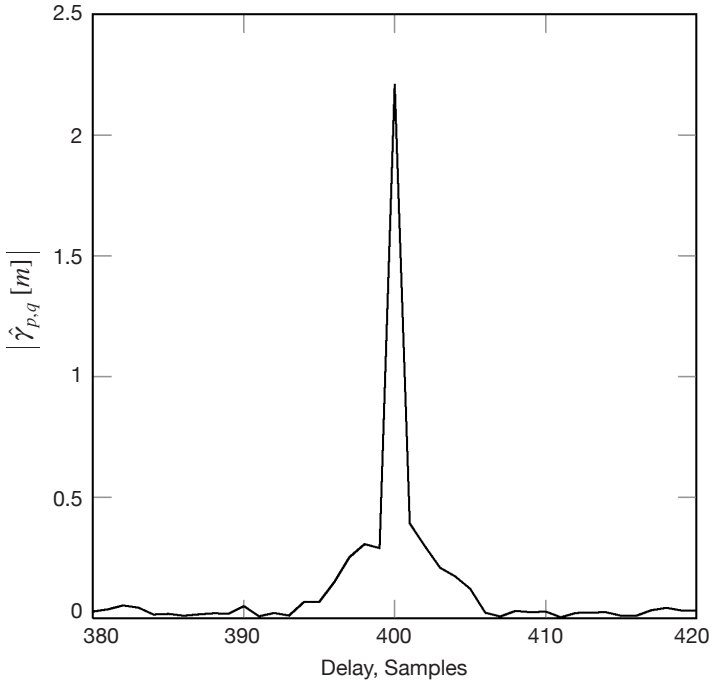

Figure 9. Magnitude of $\hat{\gamma}_{p,q}[m] = \mathcal{F}^{-1}[\hat{\Gamma}_{p,q}[r]]$. Initial delay Δ = 400 samples, $\tau' = 10^{-6}$, f_s = 1 GHz, SNR = –10 dB, $L = 2^{27}$ samples (0.125 s), K = 1024 subbands, $M = K/2$, and subband second decimation = 16.

Finally, this algorithm has been simulated jointly with the arraying scheme of Section III for two antennas with a differential delay rate of 10^{-6}, an initial delay equal to 99 subband samples, an SNR equal to 7 dB, and a QPSK signal with 100 MHz bandwidth and a roll-off factor equal to 0.9. The filter bank has been configured with 16 subbands and a decimation ratio equal to 8. The resulting combination losses are lower than 0.2 dB, and the signal to distortion ratio is above 30 dB. No transients have been detected and the demodulation of the signal has been done with the corresponding error rate to a signal to noise ratio of 10 dB.

VI. Conclusions

When combining antennas across long distances, the high delay rates among antennas cause high-differential, subband-dependent Doppler that must be compensated in order to coherently combine the antennas. Additionally, if a wide field of view is required and to reduce synchronization problems when linking remote sites, subband delay compensation must be used in addition to phase and frequency subband compensation. An algorithm to calculate the phase, delay, and delay rate between two antennas separated by large distances and subject to high delay rates has also been devised. This algorithm does not need a previous estimation of the delay rate nor a precompensation of it. Subband signals can be further decimated prior to use in the algorithm, thus reducing memory requirements and number of operations. The use of fast Fourier transform (FFT) algorithms for the calculation of the

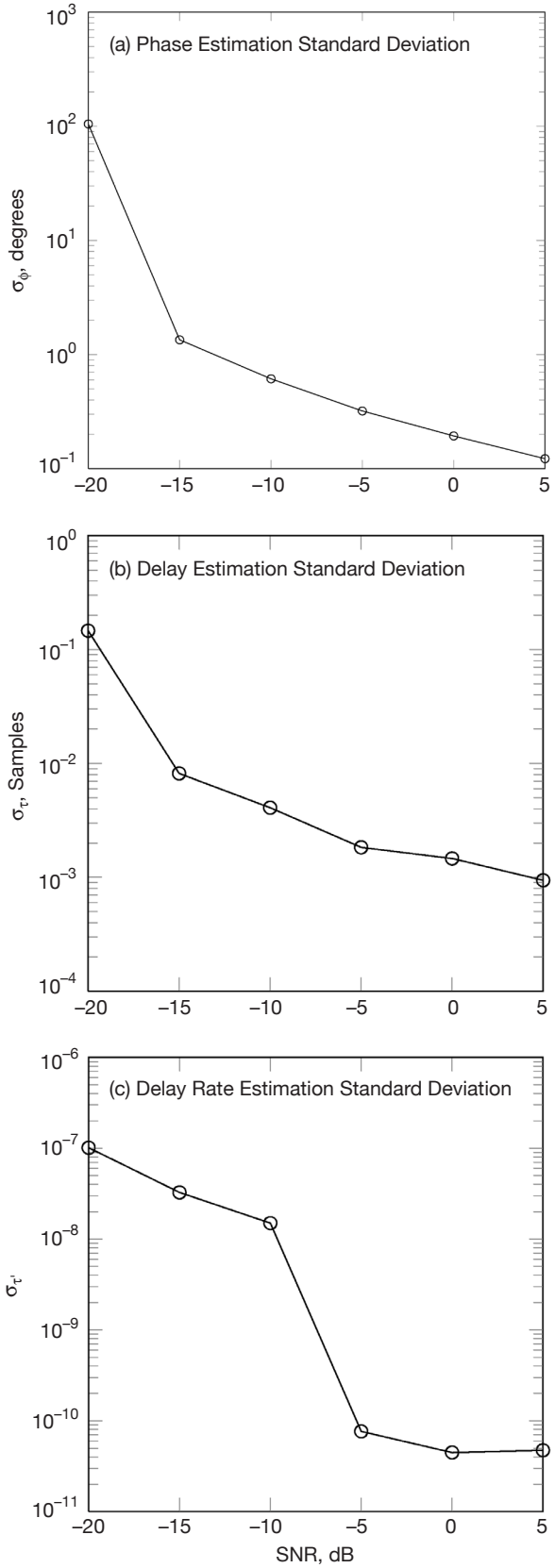

Figure 10. Bias and standard deviation of ϕ, τ, τ' estimates versus input SNR. Initial delay Δ = 400 samples, $\tau' = 10^{-6}$, f_s = 1 GHz, $L = 2^{28}$ samples (0.25 s), K = 1024 subbands, $M = K/2$, and subband second decimation = 16.

functions to be maximized allows an efficient implementation of the overall procedure. The accuracy of the algorithm at low SNR is high, due to the joint use of subband information, allowing application of the method to arrays with a large number of antenna elements, or to other applications where low SNRs are involved, such as very long baseline interferometry (VLBI) or delta-differenced one-way ranging (Delta-DOR).

References

[1] G. Shi-jian, X. Yu-lin, and C. Zeng-ping, "Study of Delay–Delay Rate 2-d Correlation in Satellite Observation of VLBI," *Proceedings of Advanced Computer Control (IACCC) 2010 2nd International Conference*, vol. 2, pp. 409–412, March 27–29, 2010.

[2] R. Navarro, "Frequency Domain Beamformer for Deep Space Network Downlink Array," *Proceedings of IEEE Aerospace Conference*, Big Sky, Montana, pp. 1–8, March 3–10, 2012.

[3] S. W. Ellingson, "Beamforming and Interference Canceling with Very Large Wideband Arrays," *IEEE Transactions on Antennas and Propagation*, vol. 51, no. 6, pp. 1338–1346, June 2003.

[4] R. E. Crochiere and R. L. Rabiner, *Multirate Digital Signal Processing*, A. V. Oppenheim, ed., Englewood Cliffs, New Jersey: Prentice-Hall, 1983.

[5] C. W. Farrow, "A Continuously Variable Digital Delay Element," *Proceedings of IEEE International Symposium on Circuits and Systems*, vol. 2, pp. 2641– 645, June 7–9, 1988.

[6] S. L. Marple, "Estimating Group Delay and Phase Delay via Discrete-Time 'Analytic' Cross-Correlation," *IEEE Transactions on Signal Processing*, vol. 47, no. 9, pp. 2604–2607, September 1999.

[7] J. Yli-Kaakinen and T. Saramaki, "Multiplication-Free Polynomial-Based FIR Filters with an Adjustable Fractional Delay," *Circuits Systems and Signal Processing*, vol. 25, pp. 265–294, 2006.

[8] H. Sun and P. De Leon, *Design Techniques for Uniform-DFT, Linear Phase Filter Banks*, Technical Report, NASA Goddard Space Flight Center, 1992.

[9] A. G. Piersol, "Time Delay Estimation Using Phase Data," *IEEE Transactions on Acoustics, Speech, and Signal Processing*, vol. ASSP-29, no. 3, pp. 471–477, June 1981.